

RSC Advances



This is an *Accepted Manuscript*, which has been through the Royal Society of Chemistry peer review process and has been accepted for publication.

Accepted Manuscripts are published online shortly after acceptance, before technical editing, formatting and proof reading. Using this free service, authors can make their results available to the community, in citable form, before we publish the edited article. This *Accepted Manuscript* will be replaced by the edited, formatted and paginated article as soon as this is available.

You can find more information about *Accepted Manuscripts* in the [Information for Authors](#).

Please note that technical editing may introduce minor changes to the text and/or graphics, which may alter content. The journal's standard [Terms & Conditions](#) and the [Ethical guidelines](#) still apply. In no event shall the Royal Society of Chemistry be held responsible for any errors or omissions in this *Accepted Manuscript* or any consequences arising from the use of any information it contains.

Electrospun flexible self-standing silica/mesoporous alumina core-shell fibrous membranes as adsorbent toward Congo red

Yan Wang, Wande Ding, Xiuling Jiao* and Dairong Chen*

School of Chemistry & Chemical Engineering, National Engineering Research Center for colloidal materials, Shandong University, Jinan 250100, P.R. China.

Flexible core-shell fibrous membranes for mesoporous alumina based adsorbent have been fabricated via the one-step coaxial electrospinning, which is accomplished by electrospinning silica as the core phase and mesoporous alumina as the shell phase. The core-shell fibers could be directly electrospun in the form of membranes. After calcinations, the mesoporous alumina shell was formed to give a high adsorption capacity, and the core fibers were dense to provide the good mechanical property of the membrane. The membranes exhibit good adsorption property toward Congo red and can keep the membrane form during the cyclic test, which is easy to handle and retrieve. The good adsorption performance, high mechanical property, easily recover and reuse characteristic of the fibrous membranes, as well as easy to scale-up fabrication process facilitate their practical application in environmental remediation.

1. Introduction

Water decontamination technology attracts more and more attention since the water contamination causes an increasing severe health risk to humankind these years.^{1,2} Organic dyes such as Congo red discharged from printing and dyeing industry are usually released into water and caused severe water contamination.² The removal of these pollutants has been investigated in various methods such as adsorption,³⁻⁶ biodegradation,⁷ chemical oxidation,⁸ and etc. Among them, the adsorption method attracts much attention due to its efficient removal of dye organics.⁹ Notably, alumina is an excellent candidate for water purification and has been widely studied as adsorbent.^{6,10-12} To date, various kinds of alumina materials including nanorod-like mesoporous alumina,⁶ hierarchical spindle-like γ -alumina materials,¹⁰ mesoporous alumina fibers¹¹ and core–corona porous structured alumina¹² have been prepared. The adsorption capacities of these materials are relatively high, but the macrographs of these materials are still limited to scattered form like powder. These materials in powder form usually suspended disperse in water and needs to filtration or centrifugation to reclaim after adsorption process, leading to the difficulty in practical application. Worse still, it may bring about the loss of adsorbents and cause the secondary pollution to the environment.^{13,14}

Recently, the fabrication of self-standing alumina films, $\text{SiO}_2@ \gamma\text{-AlOOH}$ (Boehmite) core/sheath fibrous membrane and their potential as adsorbent have been reported.^{9,15,16} However, the methods of preparing alumina films are confined to mixing the $\gamma\text{-AlOOH}$ nanofibers with suitable solvent and then dried in an oven¹⁵ or filtered,¹⁶ and the electrospinning combined hydrothermal procedure was

also reported.⁹ These preparation methods are time consuming and hard to scale-up, and the hydrothermal process is energy cost and needs demanding equipment. In addition, the flexibility and recycling performance of the alumina films have not been investigated. Besides, the γ -AlOOH particles that deposited on the electrospun silica fibers' surface via a hydrothermal method are considered to be easily come off during the application. Therefore, more efforts are needed in fabricating flexible membrane adsorbents in a simple and convenient way.

Electrospinning technique offers a simple, versatile and low-cost way for manufacturing one dimensional fibers. Notably, modeling materials to non-woven membranes that composed of continuous fibers by electrospinning method is of great value and attracts much attention these years.¹⁷⁻²⁰ However, to the best of our knowledge, there are no reports about the alumina membrane fabricated by electrospinning and being used as adsorbents. Generally, the adsorbents with higher surface area and larger pore volume are expected to have a better adsorption performance. Recently, we fabricated mesoporous alumina fibers with good adsorption performance toward Congo red.¹¹ The mesoporous alumina fibers possess large surface area, high chemical and thermal stability, but they are fragile due to their porous structure, thus the fibers cannot keep the membrane form in applications. Having considered the integrity of the membrane form and the porous structure of the fibers as well as the scalability issues, herein, we use the flexible dense silica fiber as the core and the mesoporous alumina fiber as the shell to form the silica/mesoporous alumina core-shell fibrous membranes (denoted as S/M fibrous membrane) via a coaxial electrospinning process. The

membranes show high strength attributed by the dense silica core fibers and high specific surface area derived from the mesoporous alumina shell. Therefore, the silica/mesoporous alumina fibrous membranes are flexible and exhibit good adsorption capacity as well as easy to handle and retrieve characteristics. These characteristics as well as the simple, energy-efficient and easy to scale-up preparation process make the membrane to be a good candidate in water decontamination area.

2. Experimental section

2.1. Materials

All materials were purchased commercially without any further purification, which include $\text{Al}(\text{NO}_3)_3 \cdot 9\text{H}_2\text{O}$ (analytical grade), $\text{AlCl}_3 \cdot 6\text{H}_2\text{O}$ (analytical grade), aluminum isopropoxide ($\text{Al}(\text{O}-i\text{-Pr})_3$, industrial grade), nitric acid (HNO_3 , 65 wt%, analytical grade), aluminum powder (analytical grade), polyethylene oxide (PEO, $M_w=500000$), Pluronic P123 (Poly(ethyleneglycol)-block-poly(propyleneglycol)-block-poly(ethyleneglycol)) ($\text{EO}_{20}\text{PO}_{70}\text{EO}_{20}$) ($M_w=5800$), Poly (vinyl alcohol) (PVA; M_w from 85000 to 124000 g/mol, Sigma), H_3PO_4 (analytical grade), and tetraethyl orthosilicate (TEOS; Lingfeng Chemical Co., Ltd., China).

2.2. Preparation of alumina sol

In a typical synthesis, the alumina sol with the molar composition of $\text{Al}(\text{NO}_3)_3 \cdot 9\text{H}_2\text{O}:\text{AlCl}_3 \cdot 6\text{H}_2\text{O}:\text{Al}(\text{O}-i\text{-Pr})_3:\text{Al}:\text{H}_2\text{O} = 1:1:2:4:178$ was prepared by hydrolysis and condensation under constant stirring at 80 °C. Meanwhile, appropriate amount of HNO_3 was added to the mixture to adjust the reaction rate and control the pH value of the final sol between 3.24 and 4.23. Then 0.1 g of PEO and

6.0 g of P123 were added into 40 mL as-prepared alumina sol to improve the spinnability of the sol and acted as pore structure directing reagent, respectively. The mixture was stirred for 12 h to form a spinnable sol.

2.3. Preparation of silica sol

The silica sol was synthesized according to the literature.²¹ In a typical synthesis, 22.3 mL of TEOS was added into 19.8 mL deionized water. Then 58.2 μL of H_3PO_4 was slowly added into the mixed solution under stirring. Then an equivalent weight of 10 wt% PVA solution was added into the silica sol as spinnability additive. The mixture was constantly stirred until the spinnable SiO_2 sol was obtained.

2.4. Fabrication of $\text{SiO}_2/\text{Al}_2\text{O}_3$ core-shell fibrous membrane

The silica sol and alumina sol were loaded into 10 mL plastic syringes separately. The silica sol syringe was connected to a core needle with an inner diameter of 0.4 mm and outer diameter of 0.6 mm, and the alumina sol syringe was connected to the corresponding shell needle with an inner diameter of 1.0 mm and outer diameter of 1.2 mm. The flow rates of the core and shell sol were both 2.0 mL h^{-1} . The distance between the spinneret and the aluminum collector was 17 cm and the applied voltage was 18 kV. The spinning was conducted under ambient condition. The electrospun xerogel core/shell fibrous membranes collected on the aluminum foil were dried at 90 $^\circ\text{C}$ for 12 h, and then calcined at 700 $^\circ\text{C}$, 800 $^\circ\text{C}$ or 900 $^\circ\text{C}$ for 2 h at a heating rate of 10 $^\circ\text{C}/\text{min}$.

Each of the two sols was also electrospun for comparison purpose. Details of these processes

have been presented elsewhere.^{11,21}

2.5. Characterization

The morphology of the fibers was observed by a field emission scanning electron microscopy (FE-SEM, JSM-6700F), transmission electron microscopy (TEM, JEM-1011), and high-resolution transmission electron microscope (HR-TEM, JEM-2100, accelerating voltage: 200 kV). The phase of the fibrous membranes was characterized by X-ray diffraction (XRD, Rigaku D/Max 2200PC) with CuK α radiation ($\lambda=0.15418$ nm) at room temperature, and the applied tube voltage and electric current were 40 kV and 20 mA. Thermo-gravimetric and differential scanning calorimetry (TG-DSC) measurements were characterized on a Mettler Toledo SDTA851e thermo-gravimetric analyzer with a heating rate of 10 °C min⁻¹ and up to 1200 °C in air atmosphere. The mechanical properties of the membranes were tested on a tensile tester (XG-1A, Shanghai New Fiber Instrument Co., Ltd., China) with a clamp distance of 5 mm and a drawing speed of 1 mm min⁻¹. ICP-Elemental analysis was performed on an ICP-AES (IRIS INTREPID II XSP, Thermo Electron) at a RF power of 1.15 kW and a plasma gas flow of 13.0 L min⁻¹ ($\lambda_{Al}=308.2$ nm).

The N₂ adsorption-desorption isotherms were characterized on a Quadrasorb SI apparatus. The surface area was determined via Brunauer-Emmett-Teller (BET) method, while the pore volume and pore size distribution were determined via the nonlocal density functional theory (DFT) method. All samples were degassed at 120 °C under vacuum for 12 h before analysis. The adsorption properties toward Congo red were examined by adding 10 mg samples to 5-50 mL Congo red (50 mg L⁻¹)

solution at room temperature. The concentration of Congo red was analyzed by a UV-vis spectrometer (Perkin-Elmer, Lambda-35). The characteristic absorption of Congo red at 500 nm was chosen as the monitored parameter for the adsorption process.

3. Results and discussion

3.1. Morphology and structure of the samples

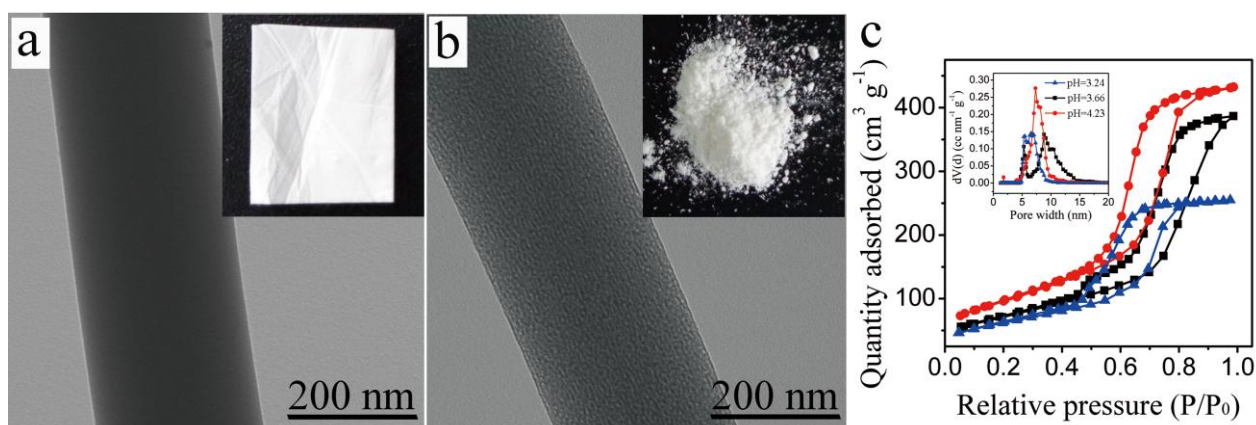


Fig. 1 TEM images of silica fibers (a), mesoporous alumina fibers (b) and N_2 adsorption-desorption isotherms of mesoporous alumina fibers with different amount of HNO_3 in the sol (c). The insets are optical graphs of the corresponding fibers (a, b) and the pore size distribution curves (c). All the fibers are calcined at 700 °C.

Fig. 1 presents the TEM images of the pure SiO_2 and Al_2O_3 fibers after calcinations at 700 °C. The silica fibers are dense and could keep the membrane form. The membrane is self-standing, flexible, and exhibit high mechanical strength (5.4 MPa),²¹ which is of great importance in practical applications. On the contrary, the mesoporous alumina fibers possess high BET surface area and large pore volume with many mesopores (Fig. 1b and Fig. 1c), which make the fibers fragile. Thus

the fibers exhibit as powder in macrograph (the inset in Fig. 1c), bringing inconvenience in practical application. However, these characteristics are in favor of their functional properties such as adsorption properties.¹¹ The formation of mesoporous alumina shell involves several processes. Firstly, the acidic aluminum sources ($\text{Al}(\text{NO}_3)_3 \cdot 9\text{H}_2\text{O}$, $\text{AlCl}_3 \cdot 6\text{H}_2\text{O}$) and alkaline aluminum sources ($\text{Al}(\text{O}-i\text{-Pr})_3$, Al powder) were hydrolyzed and polymerized in acidic solution to form the polymeric -Al-O- colloidal particles.¹¹ The optimal molar ratio of $\text{Al}(\text{NO}_3)_3 \cdot 9\text{H}_2\text{O}$ to $\text{AlCl}_3 \cdot 6\text{H}_2\text{O}$ was 1:1 from the experimental results, because the charge/size ratio of NO_3^- and Cl^- will affect the electrospinnability of the sol. Considering the hydrolysis and polymerization rate, as well as the removal of carbon during the calcination procedure, aluminum isopropoxide (easy to hydrolyze and polymerize) and aluminum powder (it hydrolyzes and polymerizes slowly and is carbon-free) were together chosen as alkaline aluminum sources. Secondly, block copolymer Pluronic P123 was added into the sol as pore structure directing reagent due to its excellent self-assembly capability to construct mesostructures.²² During the electrospinning process, the solvent was evaporated rapidly and the mesoporous structure formed via evaporation-induced self-assembly.²²⁻²⁴ Thirdly, a small amount of PEO (a common spinning additive) was added to improve the spinnability of the sol. Theoretically, the shell thickness could be controlled by adjusting the electrospinning parameters, such as the feed rates of the core and shell solutions, or the ratio of inner diameter to outer diameter of the coaxial needle. Since the adsorption property is mainly attributed to the mesoporous alumina shell, the adsorption capacity will be higher when the mesoporous alumina shell is thicker. However, the

thicker shell will reduce the tensile stress of the membranes since the core silica take an important role in maintaining the tensile stress of the membranes. Herein, we adjust the electrospinning parameters as described in the typical synthesis, in which and the membranes could meet the requirements of adsorption capacity and membrane form with a certain tensile stress simultaneously.

Usually, the adsorption capacity increases with the surface area increasing. Herein, the impacts of the precursor's pH value on the surface area and pore volume were investigated (Fig. 1c). During the first step of the precursor preparation, HNO_3 was applied to adjust the reaction rate, and the pH values of the final precursor were various with the different amount of added HNO_3 . The BET surface areas were $222.2 \text{ m}^2 \text{ g}^{-1}$, $257.1 \text{ m}^2 \text{ g}^{-1}$, $344.5 \text{ m}^2 \text{ g}^{-1}$ when the pH values of the precursor were 3.24, 3.53 and 4.23, respectively. And the corresponding pore volume were respectively $0.387 \text{ cm}^3 \text{ g}^{-1}$, $0.589 \text{ cm}^3 \text{ g}^{-1}$ and $0.655 \text{ cm}^3 \text{ g}^{-1}$. Considering the high surface area corresponds to large adsorption capacity, here the precursor with the pH value of 4.23 was chosen to fabricate the shell in the coaxial electrospinning process.

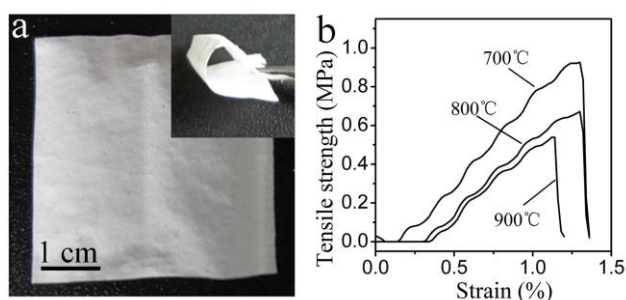


Fig. 2 The silica/mesoporous alumina fibrous membranes after calcinations at 700 °C (a) and tensile stress–strain curves of the membranes after calcinations at different temperatures (b).

The core-shell fibers could be directly electrospun in the form of membranes. During the coaxial electrospinning process, the core silica solution and the shell mesoporous alumina solution were jet out simultaneously to form a stable Taylor cone. The same solvent in the core and shell streams could lead to low interfacial tension between the two solutions, which are beneficial for the successful coaxial electrospinning.^{25,26} In the calcination process, the H_3PO_4 that added in the core solution may react with the shell alumina sol to form a small amount of aluminum phosphate at the core-shell interface, which could enhance the binding force between the core and shell and prevent the shell from coming off in application. Fig. 2a shows the optical image of the calcined membranes after bending several times. The flexibility of the membranes could be qualitative identified by the bending test as shown in the inset of Fig. 2a. The fibrous membrane keeps the integrity well and there is no cracks observed after bending the membrane several times, which favors the application of the membrane. Fig. 2b presents the mechanical properties of the core-shell membranes after calcinations at different temperatures. The tensile stress for the membranes calcined at 700 °C, 800 °C and 900 °C are respectively 0.926, 0.672 and 0.538 MPa, which are high enough to keep the integrity of the membranes during adsorption process.

The microstructure of the silica/mesoporous alumina core-shell fibers after calcinations at 700 °C are investigated by TEM. As shown in Fig. 3, the distinctive phase in the fibers could be judged by the contrast that was created by electron beam diffraction. The dark and bright regions represent the core and shell of the fibers, respectively. HRTEM was taken to give more information of the core-

shell fibers (Fig. 3b). The mesopores are obvious and distribute randomly in the shell while the core exhibits compact structure. The core-shell fibers are not completely concentric, which may be due to the inevitable whipping motion of the charged jet and bending instability during the electrospinning process. Fig. 3c presents the selected area electron diffraction (SAED) pattern of mesoporous alumina shell. The corresponding diffraction rings and weak spot on SAED pattern proved the existence of γ -alumina with low crystallinity. Moreover, the overall and localized structure of the fabricated membrane was further investigated by SEM (Fig. 4). It can be seen that the core-shell fibers are continuous with randomly distribution to form nanopores between the fibers. The high-resolution SEM image also reveals the uniform size of the fibers with the average fiber diameter of ca. 220 nm.

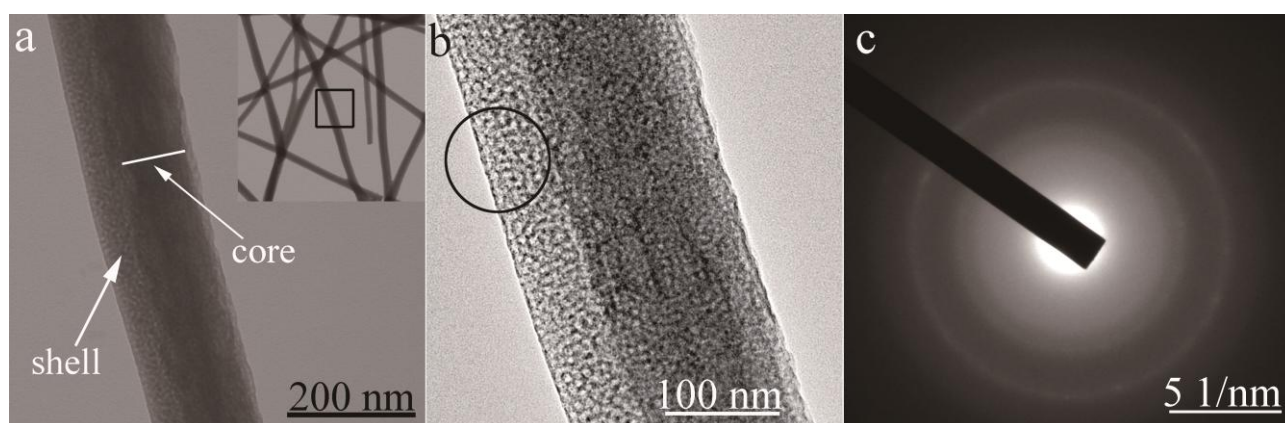


Fig. 3 TEM images (a), HR-TEM image (b) and SAED pattern of the part denoted by circle in b (c) of the silica/mesoporous alumina core-shell fibers after calcinations at 700 °C.

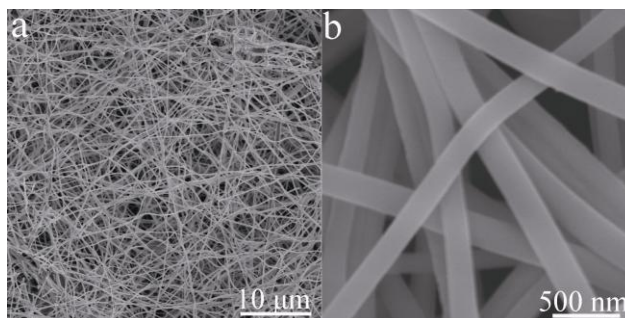


Fig. 4 SEM images of silica/mesoporous alumina fibers calcined at 700 °C at different magnification.

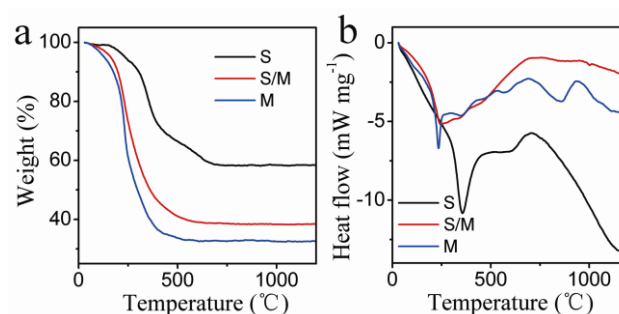


Fig. 5 TG curves (a) and DSC curves (b) of as-spun core-shell membranes and corresponding neat fibers.

The TG-DSC curves of the as-spun silica/mesoporous alumina fiber membrane have been investigated, and those of silica fiber membrane and mesoporous alumina fibers have also been presented as references (Fig. 5). The mesoporous alumina fibers and silica fiber membrane respectively show a total weight reduction of 67.28% until 600 °C and 41.59% until 700 °C. In the case of silica/mesoporous core-shell fiber membrane, the total mass loss is 61.47%, which is between that of silica fiber membrane and mesoporous alumina fibers. The content of the mesoporous alumina in silica/mesoporous alumina fibrous membrane is estimated to be 77.4% according to the following equation.

$$\text{mesoporous alumina content\%} = (W_{S/M} - W_S) / (W_M - W_S) \times 100\%$$

where $W_{S/M}$, W_S , and W_M represent the weight loss of the silica/mesoporous alumina fiber membrane, silica fiber membrane and mesoporous alumina fibers. The weight losses of the three samples all mainly derive from the removal of water, decomposition of inorganic salts and organic additives. There is no further mass loss at the temperatures higher than 700 °C. In the temperature range of 700-1000 °C, the exothermic peak in the DSC curve of mesoporous alumina fibers is attributed to the phase transformation from amorphous alumina to γ -alumina, and there is no obvious peak in curve of silica fiber membrane, which indicates that no phase transformation occurs for silica fibers from 700 to 1000 °C. The phase transformation peak for silica/mesoporous alumina fibers is weakened compared to alumina fibers, which may be caused by the curve superposition of silica fibers and mesoporous alumina fibers.

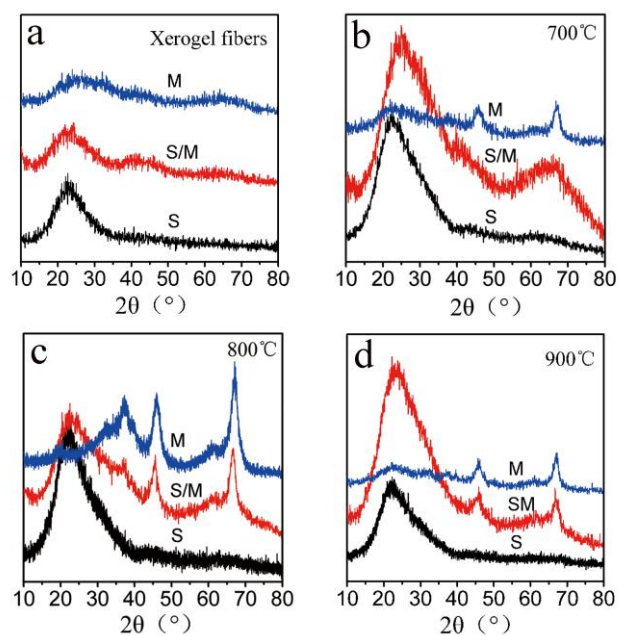


Fig. 6 XRD patterns of the xerogel core-shell fibrous membranes compared with corresponding neat fibers (a) and those calcined at 700 °C (b), 800 °C (c), 900 °C (d).

XRD was used to further illustrate the structure of the samples (Fig. 6). As for the as-spun xerogel fibers, no peaks but broad humps were observed from the XRD patterns (Fig. 6a). The results reveal that all the three types of as-spun xerogel fibers are amorphous. After calcinations at 700 °C, the peaks of γ -alumina appear in the XRD pattern of the mesoporous alumina fiber membrane while there are no obvious peaks except a broad hump observed in the pattern of the silica fiber membrane, which indicates that the amorphous alumina-based gel fibers transformed to γ -alumina fibers but the silica fibers still retain the amorphous structure after calcinations. Compared to the pure mesoporous alumina, the crystallization of γ -alumina for silica/mesoporous alumina core-shell fiber membrane is weak, which could be identified by the broad peak at 67° . The weak crystallization may be caused by the delayed effect of silica toward the crystallization of alumina. For the fibers calcined at 800 °C and 900 °C, the XRD patterns of the core-shell fibrous membranes show the reflections of γ -alumina while the silica fibrous membranes still retain the amorphous structure. The crystalline sizes of Al_2O_3 for the samples calcined at 800 °C and 900 °C have been calculated by Scherrer equation according to Scherrer line width analyses of the (440) reflections (Table 1), which are 6.9 nm and 7.2 nm, respectively.

N_2 adsorption-desorption isotherms and the corresponding pore size distributions of different samples calcined at 700 °C are presented in Fig. 7. The silica fibrous membrane shows type-III like adsorption isotherm, which represents the weak adsorption of N_2 on nonporous materials. The corresponding surface area and pore volume of the fibers are only $7.23 \text{ m}^2 \text{ g}^{-1}$ and 0.008 cc g^{-1} ,

indicating the silica fibers is compact with few pores. In the case of silica/mesoporous alumina core-shell fibrous membrane, the isotherm changes to type-IV like adsorption with H1 loop, which is similar to that of pure mesoporous alumina fibers (Fig. 1c). The results correspond with the TEM images in Fig. 3, in which the mesopores are observed apparently in the shell. The surface area and pore volume increase to $134.01 \text{ m}^2 \text{ g}^{-1}$ and 0.191 cc g^{-1} , respectively. Furthermore, the N_2 adsorption-desorption isotherms of the core-shell fibrous membranes calcined at $800 \text{ }^\circ\text{C}$ and $900 \text{ }^\circ\text{C}$ have also been investigated. As shown in Table 2, the BET surface area as well as the pore volume of the S/M fibrous membrane decreases with the calcination temperature rising. The decrease is mainly attributed to the grain growth of alumina shell at high temperature, which is consistent with our previous study.¹¹

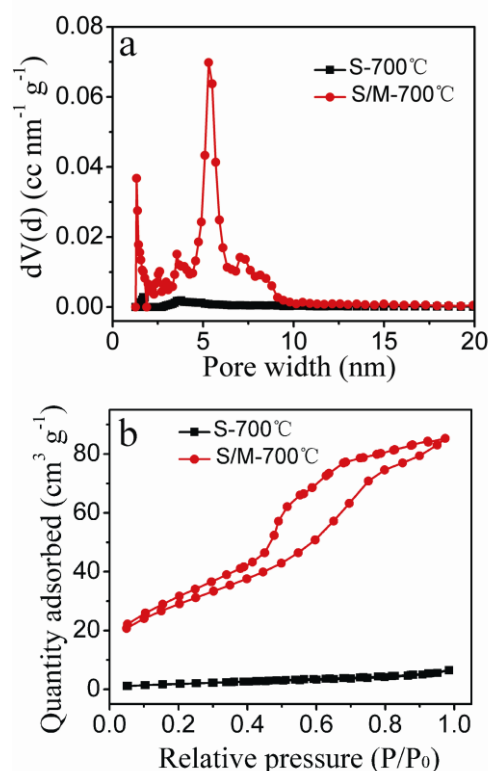


Fig. 7 N_2 adsorption-desorption isotherms of different samples after calcinations at $700 \text{ }^\circ\text{C}$ (a) and

the corresponding pore size distribution curves (b).

Table 1 The BET surface areas and porosity of the samples

Sample	crystalline size (nm)	BET surface area (m ² /g)	Pore width (nm)	Pore volume (cc/g)
S/M-700 °C	--	134.010	5.300	0.191
S/M-800 °C	6.9	104.513	5.300	0.128
S/M-900 °C	7.2	79.491	5.300	0.114

3.2. Adsorption Property toward Congo Red

The silica/mesoporous alumina fibrous membranes have potential applications in the field of water treatment as adsorbent due to the mesoporous alumina shell structure. Here, the adsorption performances of the membranes toward Congo red (a common dye) have been tested. The relative adsorption capacity was evaluated by C/C_0 (C_0 and C represent the concentrations of Congo red before and after treatment, respectively. $C_0=46 \text{ mg L}^{-1}$). As shown in Fig. 8A, the absorption peaks decreased obviously using the S/M fibrous membrane calcined at 700 °C as adsorbent, which indicates that the adsorption of Congo red on the membrane is efficient. Besides, comparative studies were carried out for adsorption toward Congo red using the neat silica fibrous membrane as adsorbent. As shown in Fig. 8B, the neat silica fibrous membrane almost has no adsorption toward Congo red even after an equilibrium time of 150 min, whereas Congo red was almost totally adsorbed on the silica/mesoporous alumina core-shell fibrous membrane with removal of ~97% Congo red ($C/C_0=0.03$) in 160 min. According to our previous study,¹¹ the adsorption of Congo red on alumina mainly depends on the electrostatic attraction and the coordination effect of the

aluminum atoms with amine groups and the sulfo groups of the Congo red. The mesoporous alumina shell possesses high surface area and large pore volume, which could provide more active sites toward Congo red. Thus, the mesoporous alumina shell plays a major role in this core-shell fibrous membrane adsorption. Furthermore, the adsorption capacity of the core-shell fibrous membrane toward Congo red is higher than those of other membrane adsorbents reported previously, such as $\text{SiO}_2@ \gamma\text{-AlOOH}$ (Boehmite) core/sheath fiber membrane⁹ and hierarchical films of layered double hydroxides.²⁷

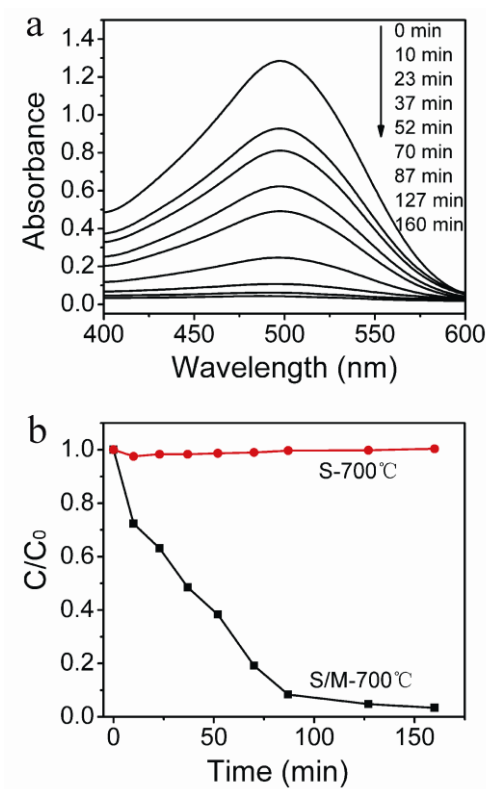


Fig. 8 UV-vis absorption spectra of Congo red in the presence of the 700 °C S/M fibrous membrane after different time intervals (A) and the adsorption rates on samples calcined at 700 °C (B). Initial Congo red concentration: 46 mg L⁻¹.

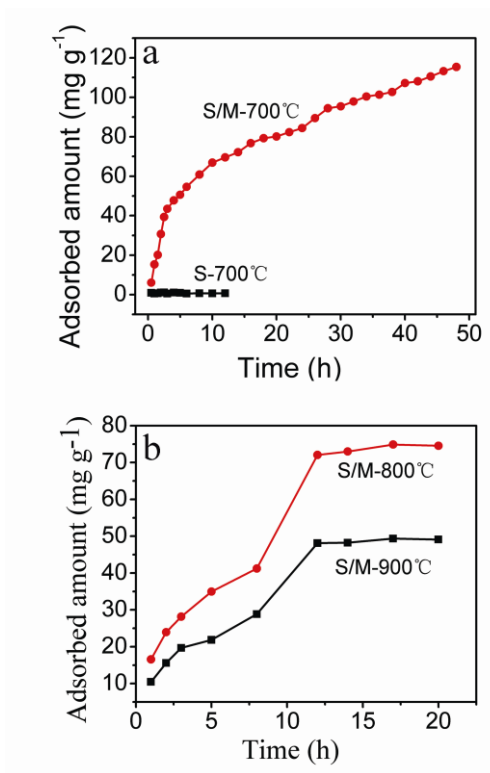


Fig. 9 The adsorption amount toward Congo red as a function of adsorption time. 6 mg membrane immersed in 50 mL Congo red solution. Initial concentration of Congo red: 55 mg/L. (A) for the membranes calcined at 700 °C, (B) for the core-shell membranes calcined at 800 and 900 °C.

To further investigate adsorbed capacity of the membrane toward Congo red, the volume of Congo red solution was further increased. As shown in Fig. 9, there was almost no adsorption for the silica fibrous membrane, while the adsorbed amount of silica/mesoporous alumina fibrous membrane continued to rise within 48 h. Considering the appropriate adsorption time in the practical application, the adsorbed amount was tested within the time limit of 48 h. The adsorbed amount of silica/mesoporous alumina fibrous membrane was 115 mg/g at 48 h, which is much higher than other membrane adsorbents reported previously, such as SiO₂@ γ -AlOOH (Boehmite) core/sheath fiber membrane toward Congo red (24.3 mg/g),⁹ self-standing alumina nanofiber film toward methyl

orange molecules (~ 10 mg/g),¹⁵ boehmite nonwovens toward stilbazo (~ 58 mg/g),¹⁶ SiO₂-TiO₂ composite porous nanofibrous membranes toward methylene blue (62.1 mg/g),¹⁸ and hierarchical films of layered double hydroxides toward Congo red (20 mg/g).²⁷ Moreover, the adsorption capacities of the core-shell membranes calcined at 800 and 900 °C toward Congo red as a function of adsorption time were also tested. As shown in Fig. 9B, the adsorption of the two samples reached equilibrium within 17 h. The saturation adsorbed amounts of the S/M-800 °C and S/M-900 °C are 74 mg/g and 49 mg/g, respectively. The adsorption capacities decreased with the calcination temperatures rising, which corresponds with the decreasing of the BET surface area.

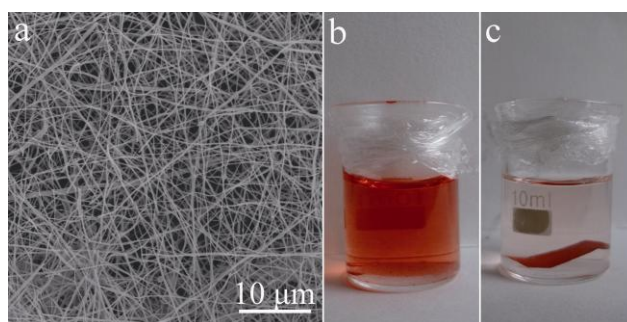


Fig. 10 SEM images of the core-shell fibrous membrane after adsorbed Congo red (a) and optical images of a Congo red before (b) and after (c) adsorption by silica/mesoporous alumina core-shell fibrous membrane.

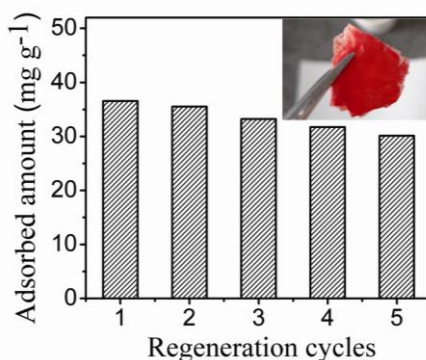


Fig. 11 Relationship between the adsorption capacity and cycle times of the S/M core-shell fibrous

membranes calcined at 700 °C. The inset is the optical images of the membranes after the fifth cycle of adsorption toward Congo red.

The silica/mesoporous alumina core-shell fibrous membrane could be manipulated and separated more conveniently due to its flexible self-standing membrane form compared to conventional powdery form, which could be seen from Fig. 10 and 11. The structure of silica/mesoporous alumina fibrous membrane after adsorbed Congo red was further investigated by SEM (Fig. 10a). The core-shell fibers are still continuous, which is good for keeping the integrity of the membrane. Furthermore, the membrane could be regenerated by a simple thermal treatment in air at 450 °C for 2 h, and the reusable property of the core-shell membrane has been investigated. The experiments were carried out by adding 10 mg membrane into 10 mL Congo red solution with an initial concentration of 55 mg/L. For the silica/mesoporous alumina fibrous membrane calcined at 700 °C, as shown in Fig. 11, the initial adsorption capacity was 36.56 mg/g, which decreased slightly with cycle times increasing and the adsorption capacity still kept as high as 30.14 mg/g even after five times of regeneration. According to our previous study, the slight decrease of the adsorption capacity for mesoporous alumina during the cyclic test may be caused by the small amount of residual SO_4^{2-} derived from Congo red, which is difficult to remove completely and thus may occupy some of the active sites of the alumina adsorbent.¹¹ The inset in Fig. 11 shows an optical photograph of the membrane that had adsorbed Congo red for the fifth cycle and dried at 70 °C for 24 h. The integrity of the membrane still kept well after being reused for several times.

To determine whether the alumina shell stable in aqueous conditions, 10 mg membrane (obtained at 700 °C) was immersed in 10 mL aqueous solution for several days, and then the Al element in the solution was analyzed on an ICP-AES apparatus. Theoretically, if all alumina in the membrane dissolved in the solution, the Al concentration in the solution should be 774 ppm. Actually, the Al content was only 0.0433 ppm from the experiment. The result shows that the alumina shell is basically stable in the aqueous conditions, and there is little dissolution of alumina shell into the water occurred. The high mechanical strength and good reusable performance in adsorption toward Congo red, as well as the high stability in aqueous solution of the membrane favors its application in water treatment.

Conclusions

In summary, the silica/mesoporous alumina core-shell fibrous membranes have been successfully fabricated through a facile and applicable one-step coaxial electrospinning technique. The calcined silica/mesoporous alumina core-shell fibrous membranes exhibit good adsorption performance toward Congo red with an adsorbed amount of 115 mg/g within 48 h. Furthermore, the silica/mesoporous alumina fibrous membranes could keep its integrity of membrane form in the reuse process, and the adsorption capacity decreased slightly after several cyclic experiments. Besides, the membrane form as adsorbent is easy to handle and reclaim in practical application. These outstanding features of the core-shell membranes favor its applications in water treatment.

Author information

Corresponding Author

*Fax: +86-531-88364281; Tel: +86-531-88364280; E-mail: jiaoxl@sdu.edu.cn

Acknowledgements

This work is supported by the National Key Technologies R&D Program (No.2013BAC01B02) and the National High-tech R&D Program (863 Program, 2012AA03A210).

References

- 1 D. W. Kolpin, E. T. Furlong, M. T. Meyer, E. M. Thurman, S. D. Zaugg, L. B. Barber and H. T. Buxton, *Environ. Sci. Technol.*, 2002, **36**, 1202-1211.
- 2 C. Chen, P. Gunawan and R. Xu, *J. Mater. Chem.*, 2011, **21**, 1218-1225.
- 3 J. B. Fei, Y. Cui, X. H. Yan, W. Qi, Y. Yang, K. W. Wang, Q. He and J. B. Li, *Adv. Mater.*, 2008, **20**, 452-456.
- 4 X. D. Chichao Yu, L. M. Guo, J. T. Li, F. Qin, L. X. Zhang, J. L. Shi and D. S. Yan, *J. Phys. Chem. C*, 2008, **112**, 13378-13382.
- 5 W. Cai, J. Yu, B. Cheng, B.-L. Su and M. Jaroniec, *J. Phys. Chem. C*, 2009, **113**, 14739-14746.
- 6 W. Cai, Y. Hu, J. Chen, G. Zhang and T. Xia, *CrystEngComm*, 2012, **14**, 972-977.
- 7 S. D. Kalme, G. K. Parshetti, S. U. Jadhav and S. P. Govindwar, *Bioresour. Technol.*, 2007, **98**, 1405-1410.
- 8 S. Chiron, A. Fernandez-Alba, A. Rodriguez and E. Garcia-Calvo, *Water Res.*, 2000, **34**, 366-377.
- 9 Y. E. Miao, R. Wang, D. Chen, Z. Liu and T. Liu, *ACS Appl. Mater. & Interfaces*, 2012, **4**, 5353-5359.
- 10 W. Q. Cai, J. G. Yu and M. Jaroniec, *J. Mater. Chem.*, 2010, **20**, 4587-4594.
- 11 Y. Wang, W. Li, X. Jiao and D. Chen, *J. Mater. Chem. A*, 2013, **1**, 10720-10726.
- 12 C. Wang, S. Huang, L. Wang, Z. Deng, J. Jin, J. Liu, L. Chen, X. Zheng, Y. Li and B.-L. Su,

- RSC Adv.*, 2013, **3**, 1699-1702.
- 13 A. S. Hashmi and G. J. Hutchings, *Angew. Chem. Int. Ed.*, 2006, **45**, 7896-7936.
- 14 Z. Guan, L. Liu, L. He and S. Yang, *J. hazard. Mater.*, 2011, **196**, 270-277.
- 15 Z.-G. Zhao, N. Nagai, T. Kodaira, Y. Hukuta, K. Bando, H. Takashima and F. Mizukami, *J. Mater. Chem.*, 2011, **21**, 14984-14989.
- 16 N. Nagai, K. Ihara, A. Itoi, T. Kodaira, H. Takashima, Y. Hakuta, K. K. Bando, N. Itoh and F. Mizukami, *J. Mater. Chem.*, 2012, **22**, 21225-21231.
- 17 F. Zhang, C. Yuan, J. Zhu, J. Wang, X. Zhang and X. W. D. Lou, *Adv. Funct. Mater.*, 2013, **23**, 3909-3915.
- 18 Q. Wen, J. Di, Y. Zhao, Y. Wang, L. Jiang and J. Yu, *Chem. Sci.*, 2013, **4**, 4378-4382.
- 19 Y. Zhu, X. Han, Y. Xu, Y. Liu, S. Zheng, K. Xu, L. Hu, and C. Wang, *ACS Nano*, 2013, **7**, 6378-6386.
- 20 M. Shang, W. Wang, S. Sun, E. Gao, Z. Zhang, L. Zhang and R. O'Hayre, *Nanoscale*, 2013, **5**, 5036-5042.
- 21 X. Mao, Y. Si, Y. Chen, L. Yang, F. Zhao, B. Ding and J. Yu, *RSC Adv.*, 2012, **2**, 12216-12223.
- 22 J. H. Pan, X. S. Zhao and W. I. Lee, *Chem. Eng. J.*, 2011, **170**, 363-380.
- 23 D. Grosso, F. Cagnol, G. J. d. A. A. Soler-Illia, E. L. Crepaldi, H. Amenitsch, A. Brunet-Bruneau, A. Bourgeois and C. Sanchez, *Adv. Funct. Mater.*, 2004, **14**, 309-322.
- 24 S. Zhan, D. Chen, X. Jiao, and C. Tao, *J. Phys. Chem. B*, 2006, **110**, 11199-11204.
- 25 J. H. Yu, S. V. Fridrikh and G. C. Rutledge, *Adv. Mater.*, 2004, **16**, 1562-1566.
- 26 D. Li, A. Babel, S. A. Jenekhe and Y. Xia, *Adv. Mater.*, 2004, **16**, 2062-2066.
- 27 Y. Zhao, S. He, M. Wei, D. G. Evans and X. Duan, *Chem. Commun.*, 2010, **46**, 3031-3033.

Graphical abstract

Flexible silica/mesoporous alumina core-shell fibrous membranes with good adsorption capacity toward Congo red have been fabricated by coaxial electrospinning method.

